University of Tehran Press

DESERT

Online Issn: 475-2345X

Home page: https://jdesert.ut.ac.ir/

Remote sensing-based monitoring of the spatiotemporal characteristics of drought using hydro-meteorological indices

Nasrin Moazami[1], Amirreza Keshtkar [1✉], Saeed Hamzeh[2], Saham Mirzaei[2], Hamidreza Keshtkar[3], Ali Afzali[4]

1- Desert Management Dept., International Desert Research Center (IDRC), University of Tehran, Tehran 1417763111, Iran. Keshtkar@ut.ac.ir, ORCID: 0000-0001-6747-2836
2- GIS & RS Dept., Faculty of Geography, University of Tehran, Tehran 1417763111, Iran
3- Faculty of Natural Resources, University of Tehran, Karaj, Iran.
4- Technology and Research Office, University of Tehran, Tehran 1417614411, Iran

Article Info

Article type:
Research Article

Article history:
Received 31 December 2021
Received in revised form 26 May 2022
Accepted 13 July 2022
Published online 25 September 2022

Keywords:
Correlation Analysis,
SPI,
NDVI,
LST

ABSTRACT

Due to climate change, drought events will probably occur more frequently and be more intense. Therefore, effective drought monitoring and assessment is vital in developing knowledge of drought, drought adaptation, and mitigatory actions. Remote sensing has been widely used for monitoring drought in recent years. In the current research, three groups of remote sensing indices, i.e. vegetation, thermal and moisture indices, were applied to determine the correlation between them and the standardized precipitation index (SPI) as drought index for the growing season (April to September) from 1999 to 2005 for rangeland areas in the Alborz province of Iran. The results indicated that normalized difference vegetation index (NDVI) (with a correlation coefficient of 0.74) and land surface temperature (LST) (with a correlation coefficient of 0.67) had the highest correlations with rainfall. Therefore, it concluded that the assumed indices are suitable for drought monitoring for this land use. Temporal analysis of the results showed that the best correlations of remote sensing indices belonged to the 6- and 9-month SPI and indicated the effect of long-term rainfall on plant growth.

Cite this article: N. Moazami, A.R. Keshtkar Khalesro, S. Hamzeh, S. Mirzaei, H.R. Keshtkar & A. Afzali (2002). Remote sensing-based monitoring of the spatiotemporal characteristics of drought using hydro-meteorological indices. DESERT, 27 (2), DOI: 10.22059/JDESERT.2022.91090

Introduction

Drought is known to be a recurrent natural phenomenon that occurs at multiple time scales and affects many regions around the world (Below *et al*., 2007; Van Loon *et al*., 2016). Simply, drought is a complex natural phenomenon that arises from a reduction in rainfall over an extended period, which causes an insufficient amount of moisture to be stored in the soil (Abbaspour and Sabetraftar, 2005; Mishra and Singh, 2010; Vurukonda *et al*., 2016; Kaisermann *et al*., 2017). Due to climate change and global warming, droughts have been observed more frequently and have been more severe in recent years, especially in arid and semi-arid regions. Alborz province is one of the most important agricultural and industrial provinces in northern Iran, and since the late 1990s, it has been affected by drought (Bazrafshan and Khalili, 2013). Increased frequency and severity of drought have had a significant impact on water resources, agricultural production, and consequently the economy across Alborz Province. Therefore, drought monitoring, assessment, and management are vital for decision makers.

Many drought indices are applied to effectively monitor and assessment drought, including the moisture index (MI) (Thornthwaite *et al*., 1955), Palmer Drought Severity Index (PDSI) (Palmer, 1965) and the Standardized Precipitation Evapotranspiration Index (SPEI) (Vicente-Serrano *et al*., 2010). Two important meteorological and hydrological indices, i.e. the Standardized Precipitation Index (SPI) (McKee *et al*., 1993) and the Standard Water Level Index (SWI) have also been used in many previous studies and were successful in quantifying the severity of short- and long-term drought for a given location and time (Guhathakurta *et al*., 2017; Halder *et al*., 2020). Because drought is a regional event, it should be monitored and evaluated on both a time and a space scale (Kogan 1997; Anderson *et al*., 2011; Hao *et al*., 2015). Remote sensing techniques are efficient and practical methods that can be applied to monitor drought in space (Toth and Jóźków, 2016). Remote sensing provides satellite observations over large regions at different temporal intervals. It systematically and continuously provides information (such as vegetation) and resolve the shortcomings of in-situ data for drought indices (Xu *et al*., 2018).

In recent years, different indices derived from remote sensing data, including vegetation, thermal, soil moisture, hydrological and meteorological ones have been applied to monitor and assess drought severity (AghaKouchak *et al*., 2015, Liu *et al*., 2020). Some popular remote sensing drought indices which are also useful for drought monitoring include the Normalized Difference Water Index (NDWI), Normalized Difference Vegetation Index (NDVI), Vegetation Condition Index (VCI), Vegetation Health Index (VHI), Anomaly of Normalized Difference Vegetation Index (NDVIA), Soil Wetness Deficit Index (SWDI), Land Surface Temperature (LST), Temperature Vegetation Dryness Index (TVDI), and Temperature Condition Index (TCI) (Kogan, 1995; Rhee *et al*.2010; Zargar *et al*., 2011; Zhang and Jia, 2013; Hao and Singh, 2015; Guo *et al*., 2018)..

Drought events occur for a variety of reasons; thus, many composite drought indices have been developed to monitor and evaluate drought by combining remote sensing drought indices, such as SMCI, VCI, PCI, TCI, etc. Some common composite drought indices are presented in Table 1. Martinez-Fernandez *et al*., (2016) assessed the SWDI index in monitoring agricultural drought and compared it with other indices, including the Crop Moisture Index and Atmospheric Water Deficit. Zhang *et al*., (2017) discussed multi-sensor frameworks and indices and assessed their ability to determine agricultural drought. Sanchez *et al*., (2018) evaluated the use of different remote sensing indices to predict agricultural drought. They reported that using remote sensing indices could provide appropriate results; however, using soil moisture indices can improve the results significantly. Six different meteorological indices for monitoring agricultural drought in the south-central USA were studied by Tian et al., (2018) and Hu *et al*., (2020) applied land surface temperature indices to monitor agricultural drought severity. Many combined drought indices have also been suggested, such as the scaled drought condition index (SDCI) (Rhee *et al*., 2010) the synthesized drought index (SDI) (Du *et al*., 2013), optimized drought indices (ODIs) (Hao *et al*., 2015), and the process-based accumulated drought index (PADI) (Zhang *et al*., 2017).

It is noteworthy that the effectiveness of these drought indices depends on regional drought monitoring, and many of them may not adequately detect the roles of single factors in the drought occurrence. Therefore, the current research applied the Pearson correlation coefficient method to compare some remote sensing indices with SPI drought index and to analyze the drought in Alborz province.

The main purposes of the current research were to evaluate the capability of single remote sensing indices in monitoring and assessing drought and to compare the correlation coefficients of remote sensing indices with SPI in monitoring meteorological drought in the Alborz province over space and time.

Table 1. Summary of some composite drought indices

Composite index	Data sources	Method	Reference
SDCI	Precipitation, LST, NDVI, reflectance	Empirical weights	(Rhee *et al*., 2010)
MIDI	Precipitation, soil moisture, and LST	Empirical weights	(Zhang and Jia, 2013)
SDI	Precipitation, LST and NDVI	Principal Component Analysis (PCA)	(Du *et al*., 2013)
MDI	Precipitation, runoff, evapotranspiration and soil moisture	Kernel PCA and kernel entropy component analysis (KECA)	(Rajsekhar *et al*., 2015)
OMDI/MVDI	Precipitation, soil moisture, LST and NDVI	Empirical weights, PCA, and constrained optimization	(Hao *et al*., 2015)
PADI	Precipitation, soil moisture, NDVI	Evolution Process-based Multi-sensor Collaboration (EPMC)	(Zhang *et al*., 2017)
MCDI	Precipitation, LST and NDVI	Multivariable Linear Regression	(Liu *et al*., 2020)

Material and methods

Study Area

The study area is Alborz province where located in the northern part of Iran over a longitude of 50°9' to 51°28' and latitude of 35°32' to 36°20', covering a total area of 5833 km^2 (Fig. 1). Annual average precipitation in Alborz is about 361 mm, and winter and summer have the highest and lowest amounts of annual precipitation with 42.3% and 5.1%, respectively. The climate of Alborz province is highly diverse, exhibiting desert climes in the southern parts and semi-humid and humid climes in the northern parts. Considering the general situation of the province, the most serious conflicts of the north-south climate are seen in the south of the province (Moazami, 2016; Pishgar-Komleh *et al*., 2017; Omid *et al*., 2018).

In recent years, Alborz province has had to cope with less precipitation and unsuitable distribution, and the frequent and severe drought events have brought about significant restrictions in production in its agricultural and rangeland regions. Thus, this study considered rangeland areas, the most common land use in Alborz province, as the most important priority in the study of drought monitoring and assessment. To this end, the study area classified into the four categories including rangeland and the other land uses (Fig. 2).

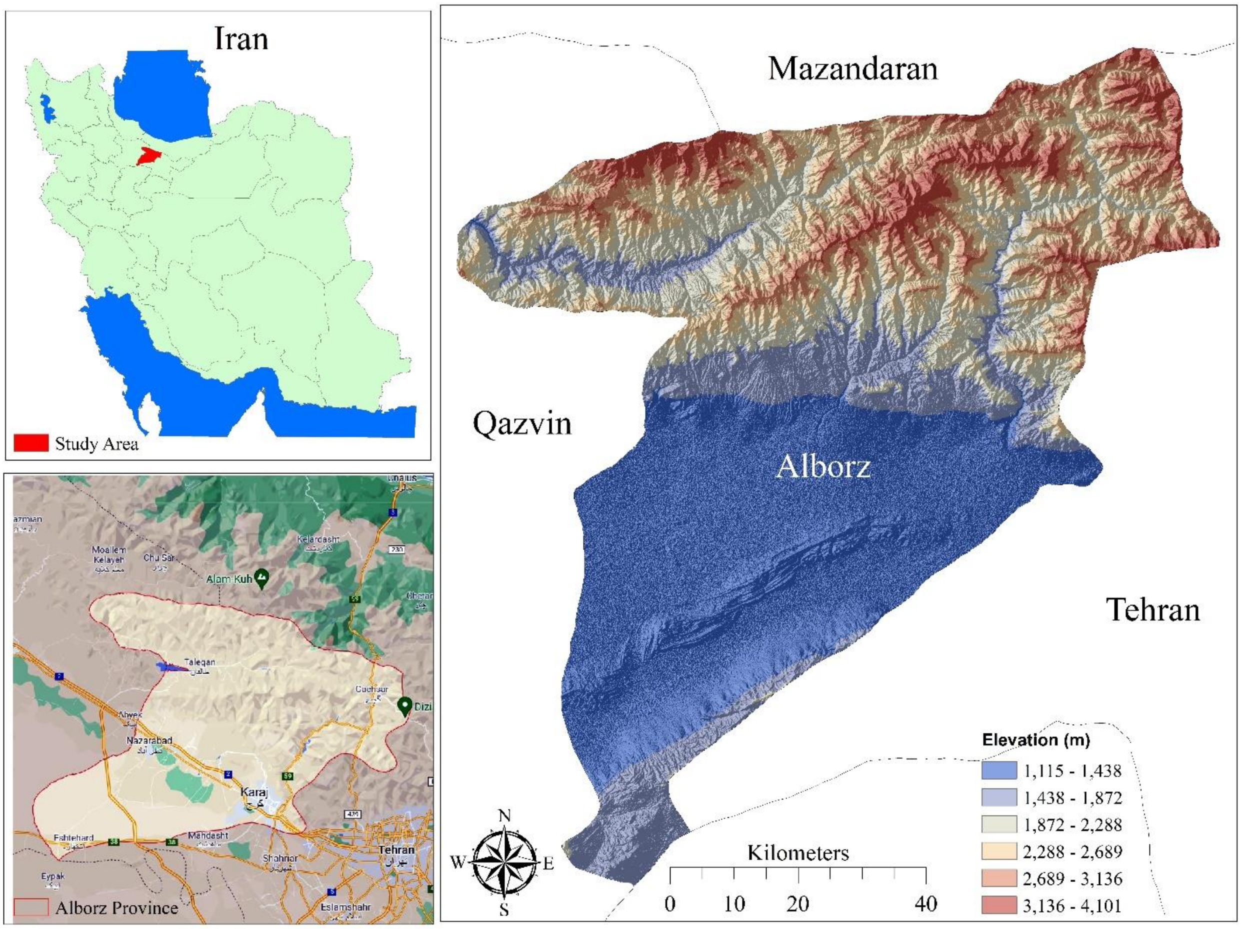

Figure 1. Geographical location and elevation model of the study area

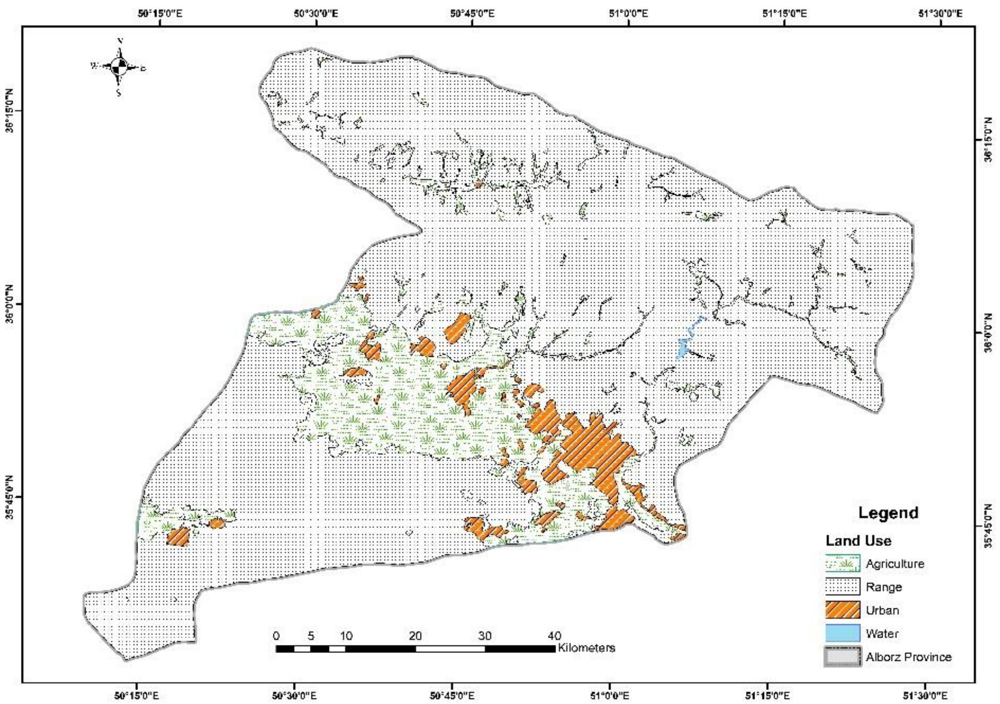

Figure 2. Classification of the study area based on land use

Satellite Data

In current research cloud free and corrected atmospheric/radiometric (L2T) satellite images of Landsat-5 TM (Thematic Mapper) with 30 m resolution were freely obtained from the United State Geological Survey (USGS; https://earthexplorer.usgs.gov). The TM data (path/row:165/35) was collected for the months of April to September during the period 1999-2005. These months was selected, because the peak growth of vegetation occurs during these times of year in the northern hemisphere (Kong *et al*., 2017). All the acquired images were projected in UTM Zone 39 N (WGS 84) and all scenes were verified for geometric accuracy. In this study, the satellite data were used to create different kind of spectral indices. Accordingly, in order to detect and monitor drought timely at study area, we investigated three groups of satellite indices: (a) vegetation, (b) thermal, and (c) soil moisture indices.

Vegetation Indices

In the current study, the applied vegetation indices included Normalized Difference Vegetation Index (NDVI), Vegetation Condition Index (VCI), Vegetation Health Index (VHI), Normalized Difference Water Index (NDWI), and Normalized Difference Vegetation Index Anomaly (NDVIA). The NDVI is the most popular vegetable index and has been used to monitor drought severity in different regions (Duan *et al*., 2017). The VCI index was determined based on the maximum and minimum NDVI values during the study period (Zambrano *et al*., 2016). The VHI index reflects the vegetation health status and is calculated based on the values of the VCI and TCI indices for the given time (He *et al*., 2018). The NDWI index shows the water content and determines the moisture stress level of the plant. This index can be calculated using near infrared (NIR) and infrared short wave (SWIR) bands (Donia *et al*., 2019). The NDVIA index expresses the difference between the NDVI values and its average value over a given period (Li *et al*., 2016). Table 2 shows the equation used to calculate these indices.

Table 2. Relation for the Vegetation Indices

Index	Relation	Reference
NDVI	$NDVI = \frac{\rho_{NIR} - \rho_{RED}}{\rho_{NIR} + \rho_{RED}}$	Ji and Peters (2003); Nouri et al. (2017)
VCI	$VCI = \frac{NDVI_{ijk} - NDVI_{i\,min}}{NDVI_{i\,max} - NDVI_{i\,min}}$	Kogan (1995, 2001)
VHI	$VHI = r_1 \times VCI_{ijk} + r_2 \times TCI_{ijk}$	Gao (1996)
NDWI	$NDWI = \frac{\rho_{NIR} - \rho_{SWIR}}{\rho_{NIR} + \rho_{SWIR}}$	Gao (1996)
NDVIA	$NDVIA = \overline{NDVI_{ij}} - NDVI_{ijk}$	Anyamba et al (2001)

Where ρ_{RED} is the reflection of the red spectrum. ρ_{NIR} and ρ_{SWIR} show the reflections near infrared spectrum and near short-wave infrared spectrum, respectively. $NDVI_{ijk}$ is the monthly $NDVI$ value for pixel i in month j and year k. $NDVI_{i\,max}$ and $NDVI_{i\,min}$ are the maximum and minimum values of the multi-year NDVI for pixel i, respectively. VCI_{ijk} and TCI_{ijk} are the monthly VCI and TCI values for pixels i in month j and year k, respectively. r_1 and r_2 are the weights of VCI and TCI (in the most similar researches, they were considered to be 0.5). $\overline{NDVI_{ij}}$ is the average value of the NDVI index for pixel i in month j.

Thermal Indices

This research used the two thermal indices of land surface temperature (LST) and temperature confidence index (TCI). From among the different methods for calculating LST using thermal infra-red data, this study used a single-band method. To determine the LST, the brightness temperature must be calculated. Thus, the thermal infrared data must first be converted into radiation using Planck law (Zare *et al*., 2020).

$$T_b = \frac{k_2}{\ln(\frac{k_1}{l\lambda}+1)} \quad (1)$$

Where T_b is the brightness temperature, $l\lambda$ is the spectral radiation in $Wm^{-2}\mu m^{-1}sr^{-1}$, and k_1 and k_2 are the calibration coefficients with dimension $Wm^{-2}\mu m^{-1}sr^{-1}$.
Calculating the TCI also needs the brightness temperature. High temperature or low TCI indicates drought severity. Due to the fact that increasing in surface temperature is earlier than vegetation decline during drought periods, it seems that this group of indices is useful for assessing the drought severity in plant-covered areas (Shao-E *et al*. 2010). Table 3 illustrates the equation for calculating these indices.

Table 3. Relations for the Thermal Indices.

Index	Relation	Reference
LST	$LST = \frac{T_b}{[1+\left(\frac{\lambda T_b}{\alpha}\right)\ln\varepsilon]}$	Artis and Carnahan (1982)
TCI	$TCI_{ijk} = \frac{(BT_{ijk} - BT_{i\,min})}{(BT_{i\,max} - BT_{i\,min})}$	Kogan (1995, 2001)

Where LST is the surface temperature, T_b is the brightness temperature, λ is the wavelength of the radiation, ε is the radiation power and $\alpha = hc/k$ (h is the Planck's constant, c is the speed of light and k is the Boltzmann's constant). BT_{ijk} is the brightness temperature for pixel i in month j and year k, $BT_{i\,max}$ and $BT_{i\,min}$ are the maximum and minimum brightness temperatures for pixel i in a particular period.

Soil Moisture Indices

This study used the two common soil moisture indices of soil wetness deficit index (SWDI) and temperature-vegetation dryness index (TVDI). These indices show the relationship between soil temperature, vegetation and soil moisture in a range between zero and one. The SWDI index has a direct correlation with soil moisture, but the TVDI index indicates an inverse relationship (Sayago *et al*., 2017). Table 4 shows the equation for these indices.

Table 4. Relations for the Soil Moisture Indices

Index	Relation	Reference
SWDI	$SWDI = \frac{T_{\max(i)} - T_{s(i)}}{T_{\max(i)} - T_{min(i)}}$	Verstraeten (2006); Mallick et al. (2009)
TVDI	$TVDI = \frac{LST - LST_{min}}{LST_{max} - LST_{min}}$	Sandholt et al. (2002)

Where i is the pixel number, $T_{s(i)}$ is same as the LST for pixel i, $T_{min(i)}$ and $T_{\max(i)}$ are the minimum and maximum observed temperatures for pixel i, respectively.

Meteorological data

Data on daily precipitation from 1973 to 2013 for the study area were obtained from the Iran Meteorological Organization, and no data was missing for the study area. There are 33 weather stations in Alborz province.

The SPI index was presented in 1993 by McKee *et al*., (1993). It was designed to quantify precipitation deficit at multiple time scales. The SPI index is calculated using Equation 2.

$$SPI = \frac{p_i - \bar{p}}{SD} \quad (2)$$

Where p_i the rainfall amount is during the desired period at the i^{th} station, $\bar{p}$ is the average rainfall at the i^{th} station and SD is the standard deviation of the i^{th} station's rainfall. Long-term rainfall data (over 30 years) must be used to calculate the SPI. Thus, the meteorological data (including daily and monthly rainfall) was collected from three synoptic stations and 30 rain-gauge stations in the study area. Some stations, however, had been established less than 30 years ago. Therefore, only 10 rain-gauge stations with sufficient data were selected for data collection, and the SPI indices for the periods of 1, 3, 6, 9, 12, and 24 months were calculated for the years 1973 to 2013. Moreover, annual SPI indices were calculated to determine the driest and wettest years.

Data analysis

The relationships between data can be investigated in different ways. One method is correlation analysis. Generally, correlation analysis determines type and severity between two sets of data. In the popular Pearson correlation analysis, the result is declared as a correlation coefficient named r, the value of which is between –1 to +1, such that 0 means there is no correlation between data. Positive values indicate a direct correlation between data, and negative values indicate an indirect correlation (Rahimzadeh Bajgiran *et al*., 2008).

After the data collection process, the correlation between remote sensing indices and meteorological drought index were calculated, and the results were analyzed for rangeland area. The best index and the best time scale for drought monitoring were determined, and then drought zoning maps were represented using the Kriging method (Kleijnen, 2017).

Results and Discussion

Correlations between SPI and remote sensing indices

The remote sensing index values were calculated based on weather station locations during the research period. To evaluate the efficiency of single remote sensing indices in drought monitoring and assessment, the correlation coefficients (r) were computed between each single remote sensing drought index and the SPI in the study area.

According to the annual SPI values, the driest and wettest years were identified as 2000 and 2005, respectively. Thus, the correlation coefficients were calculated between SPIs and remote sensing indices for these years for rangelands. The results for the driest year are shown in Table 5.

Table 5 indicates that NDVI (r=0.74) and TCI (r=-0.79) indicated the highest r with SPI-12 in rangeland areas. TCI was the most sensitive in monitoring long-term drought compared with other remote sensing indices, and again the r decreased as the SPI time scale decreased. Results showed that for the SPI short-time scale, TCI and NDWI had the highest r with SPI-3 compared to other indices in rangeland areas. This suggests that TCI and NDWI are able to provide valid and considerable but time-lagged information in meteorological and vegetation drought monitoring and assessment. For SPI-1, the results showed that VCI and VHI had the highest r in rangeland areas. The results also indicated that NDVIA showed the highest r with SPI-24 compared to other SPI time scales in both types of land use. LST showed the highest r with SPI-24 in rangeland areas. The values of r between NDWI and LST in rangeland areas were lower than those between other remote sensing indices and SPIs. NDWI and SPI-12 and LST and SPI-6 showed higher r values than between NDWI, LST and other SPIs, which suggests that the drought information reflected in NDWI was lagged for a longer time than in LST. The results for the wettest year are shown in Table 6.

Table 5. Correlation between different time scale SPIs and single remote sensing indices for rangelands in the study area for the driest year (2000)

		SPI1	SPI3	SPI6	SPI9	SPI12	SPI24
Rangelands	NDVI	0.2987	0.1332	0.3856	0.7021	0.7419	0.5222
	VCI	-0.4274	0.0794	-0.1262	-0.4220	-0.5086	-0.3984
	VHI	-0.4083	-0.1522	-0.3664	-0.5875	-0.6495	-0.5174
	NDWI	-0.0020	-0.3228	-0.3890	0.3746	0.5232	0.3371
	NDVIA	-0.0500	-0.1676	-0.0510	-0.0360	-0.1742	-0.3324
	LST	-0.0421	-0.2909	-0.2214	-0.1582	-0.1179	-0.3424
	TCI	-0.2939	-0.4668	-0.6202	-0.6978	-0.7945	-0.5473
	SWDI	0.0417	0.2908	0.2210	0.1573	0.1169	0.3418
	TVDI	-0.0417	-0.2908	-0.2210	-0.1573	-0.1169	-0.3418

Table 6. Correlation between different time scale SPIs and single remote sensing indices for rangelands in the study area for the wettest year (2005)

		SPI1	SPI3	SPI6	SPI9	SPI12	SPI24
Rangelands	NDVI	-0.0870	-0.1701	0.0916	0.3266	0.2840	-0.0883
	VCI	-0.4671	-0.1959	-0.3244	-0.8724	-0.6236	-0.6504
	VHI	-0.4453	-0.2380	-0.4472	-0.7102	-0.7410	-0.5999
	NDWI	0.4288	0.0730	0.0732	0.2713	0.3148	0.3940
	NDVIA	0.3195	0.2224	0.2956	0.2431	0.3095	0.5009
	LST	-0.1670	-0.4824	-0.6761	-0.5299	-0.5291	-0.5532
	TCI	-0.1525	-0.2495	-0.5148	-0.6829	-0.6550	-0.1645
	SWDI	0.1670	0.4822	0.6753	0.5288	0.5280	0.5529
	TVDI	-0.1670	-0.4822	-0.6753	-0.5288	-0.5280	-0.5529

Table 6 shows that VHI (r=-0.74) and VCI (r=-0.87) showed the highest r with SPI-12 and SPI-9 in rangelands, which indicated that VHI was the most sensitive in monitoring long-term drought compared with other remote sensing indices. Moreover, the r decreased as the SPI time scale decreased. Among thermal indices, TCI (r=-0.68) showed the highest r with SPI-9 in rangeland areas. Among soil moisture indices, SWDI (r=0.67) and TVDI (r=-0.67) showed the highest r with SPI-6 in rangeland areas. The results indicated that for the SPI short-time scale, VCI and LST had the highest r with SPI-1 and SPI-3 compared to other indices in rangeland land use. For the long-time scale, VHI and VCI showed higher r values with both SPI-12 and SPI-24 in rangelands. The r values between NDWI and SPIs were lower than those between other remote sensing indices and SPIs. NDWI and SPI-1 and VHI and SPI-12 showed higher r values than those between NDWI, VHI, and other SPIs, which suggested that the drought information reflected in VHI was lagged for a longer time than that in NDWI. The NDWI index indicates the moisture content of the vegetation cover; therefore, lower NDWI values indicate moisture stress in vegetation. In 2005, when the amount of precipitation was higher, this index showed the best correlation with SPI. During droughts, increases in surface temperature occur earlier than vegetation loss. The results showed that in the driest year, increasing surface temperatures of the leaves can determine plant moisture stress and the start of drought periods well. This heat reaction occurs even when plants are well-grown. It seems that considering an index that can assess the earth surface temperature for drought monitoring will lead to better results. In the present study, the results showed that the TCI index can show drought severity well, because vegetation density is less in rangeland regions than in agricultural regions, and there are also gaps between plants. Generally, it can be said that dense vegetation decreases surface temperature, and consequently, areas with dense vegetation have lower surface temperatures (Remote Sensing of Energy Fluxes and Soil Moisture Content, edited by George P. Petropoulos, 2014, Taylor & Francis Group, NW, pp 233-245).

Temporal correlation between SPI and remote sensing indices

Figure 3 illustrates the correlation between SPI and remote sensing indices in rangeland areas. In general, remote sensing indices did not show a satisfactory correlation with SPI in rangeland areas except for NDVI. The results showed that the NDVI had the highest correlations with SPI-9 and 12. The LST index showed a satisfactory correlation with SPI in April and May.

Figure 3. Correlation between SPIs and remote sensing indices in rangelands for the driest year (2000)

Comparison of SPI Zoning with Remote Sensing Indices

Figure 4 showed that SPI for the driest year (2000) was negative, indicating greater drought severity. The results showed that most of the study area, except for the northeastern part, had low precipitation and was faced with drought. SPI zoning for June 2005 as the wettest year is shown in Figure 5. In the wettest year, most parts of the study area, except the east and south areas did not experience drought.

According to the SPI values for 2000, there was a shortage of precipitation and, consequently, a drought event in most areas of the study region except for the northeastern part. The NDWI showed normal conditions in all parts of the research area. The NDVIA and TCI indices did not correlate well with SPI, but LST showed temperature changes in different regions. Results for this index showed that the northeastern parts of the Alborz province had lower temperatures. Soil moisture indices showed strong correlations with SPI. In general, the LST, SWDI, and TVDI indices showed a significant correlation with SPI in 2000. Based on SPI values in the wettest year (2005), most areas did not experience drought events except those in the eastern parts. The NDVIA also showed normal conditions in almost all parts of the study area. Clearly, vegetation and soil moisture indices were well correlated with SPI in the wettest year.

Conclusion

In the current research, the ability of remote sensing single drought indices to monitor and detect spatial and temporal drought events in arid and semi-arid rangelands in Alborz province during the growing season was assessed. The results showed that most remote sensing indices in the study area had significant correlations with SPI drought index in long-term scales. It was concluded that LST index was the best index for rangeland areas. This result is compatible with the findings of studies by Mishra *et al*., (2017), Xu *et al*., (2018) and Park *et al*. (2017). Vegetation and thermal indices had high correlations with SPI. This finding is similar to the results obtained by Heydari *et al*. (2018) and Bento *et al*. (2018). The results of the ability assessment of single drought indices in monitoring drought indicated that these indices could determine the driest and wettest years well, especially for rangelands.

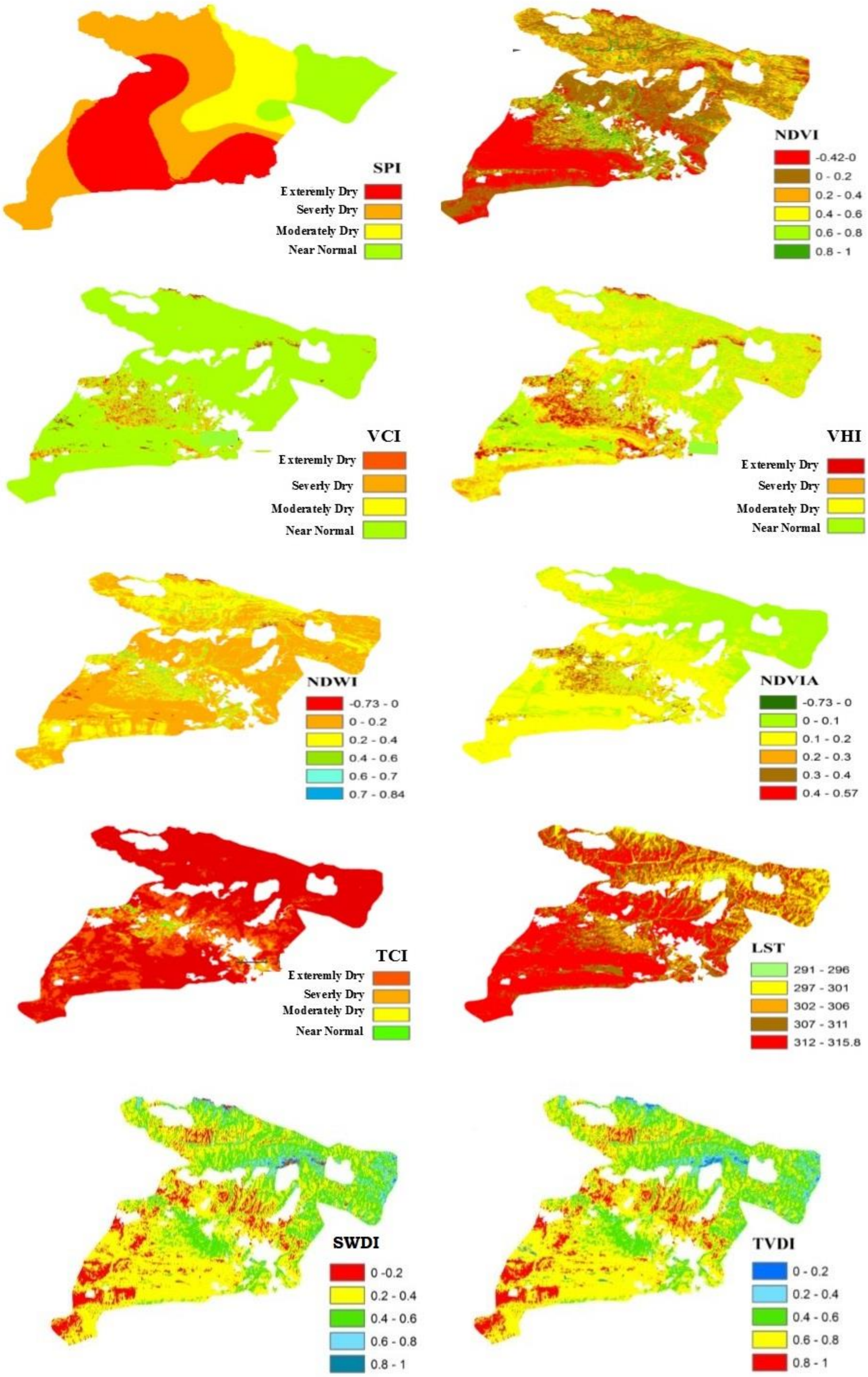

Figure 4. Drought severity by SPI, NDVI, VCI NDWI, NDVIA, TCI, LST SWDI, TVDI, and VHI indices for May in the driest year (2000)

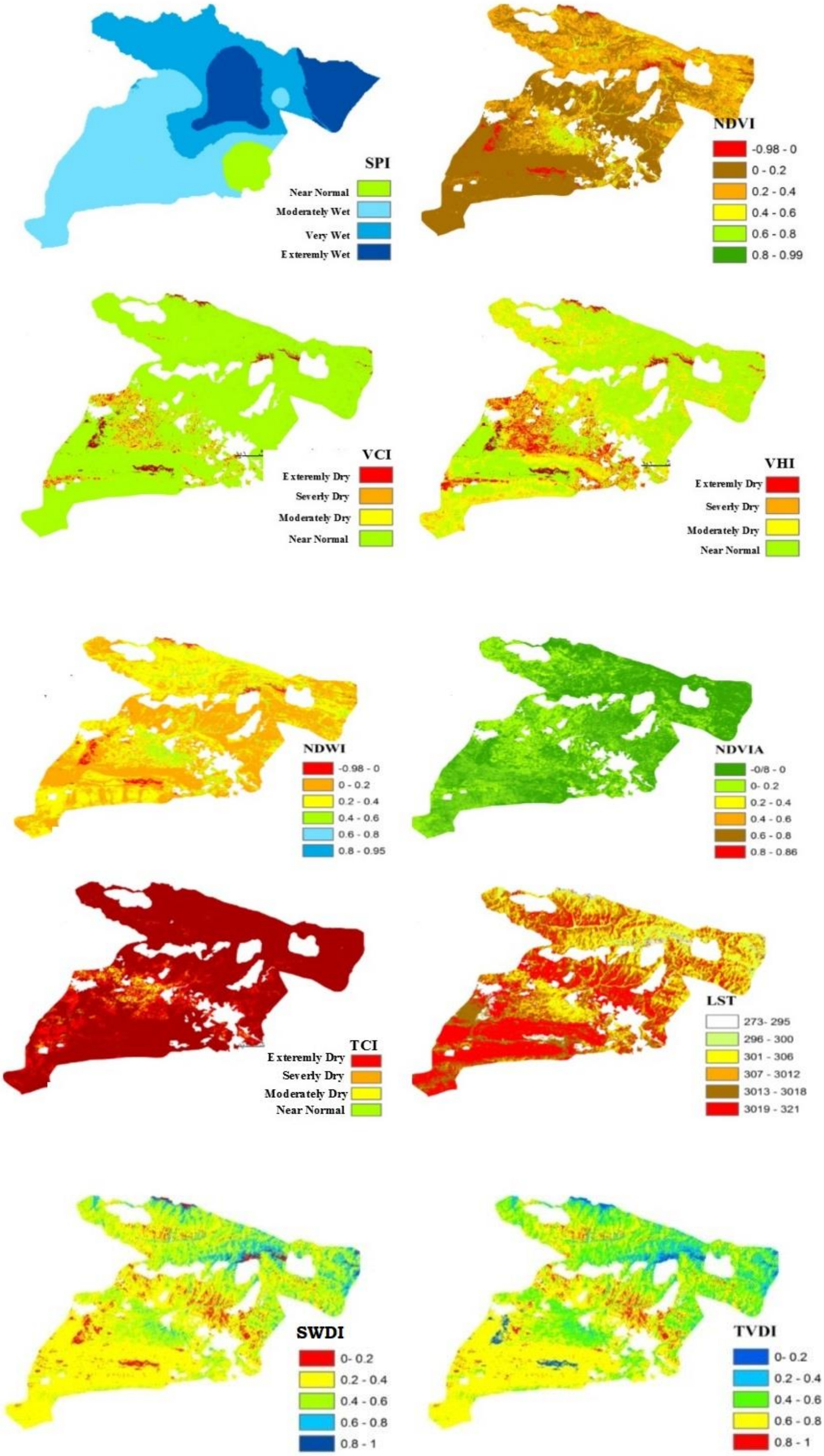

Figure 5. Drought severity by SPI, NDVI, VCI NDWI, NDVIA, TCI, LST SWDI, TVDI, and VHI indices for June in the wettest year (2005)

References

Abbaspour M, Sabetraftar A. 2005. Review of cycles and indices of drought and their effect on water resources, ecological, biological, agricultural, social and economic issues in Iran. Int J Environ Stud 62: 709–724. https://doi.org/10.1080/00207230500288968.

AghaKouchak A, Farahmand A, Melton FS, Teixeira J, Anderson MC, Wardlow BD, Hain CR. 2015. Remote sensing of drought: progress, challenges and opportunities. Geophys Rev. https://doi.org/10.1002/2014RG000456.

Almamalachy YS, Al-Quraishi AMF, Moradkhani H. 2020. Agricultural drought monitoring over Iraq utilizing MODIS products. Environ. Remote Sens GIS Iraq 10: 253–278, https://doi.org/10.1007/978-3-030-21344-2_11.

Anderson MC, Hain C, Wardlow B, Pimstein A, Mecikalski JR, Kustas WP. 2011. Evaluation of drought indices based on thermal remote sensing of evapotranspiration over the continental United States. J Clim 24: 2025-2044. https://doi.org/10.1175/2010JCLI3812.1.

Anyamba A, Tucker CJ, Eastman JR. 2001. NDVI anomaly patterns over Africa during the 1997/98 ENSO warm event. Int J Remote Sens 22: 1847–1860. https://doi.org/10.1080/01431160010029156.

Artis DA. 1982. Carnahan WH Survey of emissivity variability in thermography of urban areas. Remote Sens Environ 12: 313–329. https://doi.org/10.1016/0034-4257 (82)90043-8.

Bazrafshan J, Khalili A. 2013. Spatial Analysis of Meteorological Drought in Iran from 1965 to 2003. Desert 18: 63-71.

Below R, Grover-Kopec E, Dilley M. 2007. Documenting drought-related disasters: A global reassessment. J Environ. Dev 16: 328–344. https://doi.org/10.1177%2F1070496507306222.

Bento VA, Gouveia CM, DaCamara CC, Trigo IF. 2018. A climatological assessment of drought impact on vegetation health index. Agric. for Meteorol 259: 286–295. https://doi.org/10.1016/j.agrformet.2018.05.014.

Bhuiyan C. 2004. Various drought indices for monitoring drought condition in Aravalli terrain of India. Proc XXth ISPRS Congr, Istanbul, Turkey, pp 12–23.

Chezgi J, Pourghasemi HR, Naghibi SA, Moradi HR, KheirkhahZarkesh M. 2016. Assessment of a spatial multi-criteria evaluation to site selection underground dams in the Alborz Province, Iran. Geocarto Int 31: 628–646. https://doi.org/10.1080/10106049.2015.1073366.

Donia N. 2019. NDWI Based Change Detection Analysis of Qarun Lake Coastal Area, El-Fayoum, Egypt. Adv Remote Sens Geo Informatics Appl 25: 121–124. https://doi.org/10.1007/978-3-030-01440-7_29.

Du L, Tian Q, Yu T, Meng Q, Jancso T, Udvardy P, Huang Y. 2013. A comprehensive drought monitoring method integrating MODIS and TRMM data. J Appl Earth Obs Geoinf Int 23: 245-253. https://doi.org/10.1016/j.jag.2012.09.010.

Duan T, Chapman SC, Guo Y, Zheng B. 2017. Dynamic monitoring of NDVI in wheat agronomy and breeding trials using an unmanned aerial vehicle. F Crop Res 210: 71–80. https://doi.org/10.1016/j.fcr.2017.05.025.

Gao B-C. 1996. NDWI-A normalized difference water index for remote sensing of vegetation liquid water from space. Remote Sens Environ 58: 257–266.

Guo H, Bao A, Liu T, Jiapaer G, Ndayisaba F, Jiang L, Kurban A, De Maeyer P. 2018. Spatial and temporal characteristics of droughts in Central Asia during 1966–2015. Sci Total Environ 624, 1523–1538. https://doi.org/10.1016/j.scitotenv.2017.12.120.

Guhathakurta P, Menon P, Inkane PM, Krishnan U, Sable ST. 2017. Trends and variability of meteorological drought over the districts of India using standardized precipitation index. J Earth Syst Sci 126: 120-140. https://doi.org/10.1007/s12040-017-0896-x.

Halder S, Roy MB, Roy PK. 2020. Analysis of groundwater level trend and groundwater drought using Standard Groundwater Level Index: a case study of an eastern river basin of West Bengal, India, SN. Appl Sci 2: 1–24. https://doi.org/10.1007/s42452-020-2302-6.

Hao Z, Singh VP. 2015. Drought characterization from a multivariate perspective: A review. J Hydrol 527: 668–678. https://doi.org/10.1016/j.jhydrol.2015.05.031.

Hao C, Zhang J, Yao F. 2015. Combination of multi-sensor remote sensing data for drought monitoring over Southwest China. J Appl Earth Obs Geoinf Int 35: 270-283. https://doi.org/10.1016/j.jag.2014.09.011.

He Z, Vorogushyn S, Unger-Shayesteh K, Gafurov A, Kalashnikova O, Hagenlocher M. 2018. Attribution of vegetation health index (VHI) changes to runoff changes in headwater catchments in the Chu river basin, Central Asia. EGU Gen Assem Conf Abstr, pp 86-100.

Heydari H, ValadanZoe, M, Maghsoudi Y, Dehnavi S. 2018. An investigation of drought prediction using various remote-sensing vegetation indices for different time spans. Int J Remote Sens 39: 1871–1889. https://doi.org/10.1080/01431161.2017.1416696.

Hu T, Renzullo LJ, VanDijk AIJM, He J, Tian S, Xu Z. 2020. Monitoring agricultural drought in Australia using MTSAT-2 land surface temperature retrievals. Remote Sens Environ 236: 111-119. https://doi.org/10.1016/j.rse.2019.111419.

Ji L, Peters AJ. 2003. Assessing vegetation response to drought in the northern Great Plains using vegetation and drought indices. Remote Sens Environ 87: 85–98. https://doi.org/10.1016/S0034-4257(03)00174-3.

Kaisermann A, de Vries FT, Griffiths RI, Bardgett RD. 2017. Legacy effects of drought on plant–soil feedbacks and plant–plant interactions. New Phytol 215: 1413–1424. https://doi.org/10.1111/nph.14661.

Kleijnen JPC. 2017. Regression and Kriging metamodels with their experimental designs in simulation: a review. Eur J Oper Res 256: 1–16. https://doi.org/10.1016/j.ejor.2016.06.041.

Kogan FN. 1995. Application of vegetation index and brightness temperature for drought detection. Adv Sp Res 15: 91–100. https://doi.org/10.1016/0273-1177(95)00079-T.

Kogan FN. 1997. Global drought watch from space. Bull Am Meteorol Soc 78: 621–636. https://doi.org/10.1175/1520-0477(1997)078<0621:GDWFS>2.0.CO;2.

Kogan FN. 2001. Operational space technology for global vegetation assessment. Bull Am Meteorol Soc 82:1949–1964.https://doi.org/10.1175/1520-0477(2001)082%3C1949:OSTFGV%3E2.3.CO;2.

Kong D, Zhang Q, Singh VP, Shi P. 2017. Seasonal vegetation response to climate change in the Northern Hemisphere (1982–2013). Glob Planet Change 148: 1–8. https://doi.org/10.1016/j.gloplacha.2016.10.020.

Li R, Zhao T, Shi J. 2016. Index-based evaluation of vegetation response to meteorological drought in Northern China. Nat Hazards 84: 2179–2193. https://doi.org/10.1007/s11069-016-2542-3.

Liu X, Zhu X, Pan Y, Li S, Liu Y, Ma Y. 2016. Agricultural drought monitoring: Progress, challenges, and prospects. J Geogr Sci 26: 750–767. https://doi.org/10.1007/s11442-016-1297-9.

Liu Q, Zhang Sh, Zhang H, Bai Y, Zhang J. 2020. Monitoring drought using composite drought indices based on remote sensing. Science of the Total Environment 711: 1-10. https://doi.org/10.1016/j.scitotenv.2019.134585

Mallick K, Bhattacharya BK, Patel NK. 2009. Estimating volumetric surface moisture content for cropped soils using a soil wetness index based on surface temperature and NDVI. Agric for Meteorol 149: 1327–1342. https://doi.org/10.1016/j.agrformet.2009.03.004.

Martínez-Fernández J, González-Zamora A, Sánchez N, Gumuzzio A, Herrero-Jiménez CM. 2016. Satellite soil moisture for agricultural drought monitoring: Assessment of the SMOS derived Soil Water Deficit Index. Remote Sens Environ 177: 277–286. https://doi.org/10.1016/j.rse.2016.02.064.

McKee TB, Doesken NJ, Kleist J. 1993. The relationship of drought frequency and duration to time scales. Proc 8th Conf Appl Climatol Boston, pp 179–183.

Mesgaran MB, Madani K, Hashemi H, Azadi P. 2017. Iran’s land suitability for agriculture. Sci Rep 7: 1–12. https://doi.org/10.1038/s41598-017-08066-y.

Mishra A, Vu T, Veettil AV, Entekhabi D. 2017. Drought monitoring with soil moisture active passive (SMAP) measurements. J Hydrol 552: 620–632. https://doi.org/10.1016/j.jhydrol.2017.07.033.

Mishra AK, Singh VP. 2010. A review of drought concepts. J Hydrol 391: 202–216. https://doi.org/10.1016/j.jhydrol.2010.07.012.

Moazami N. 2016. Drought monitoring and analysis using remote sensing indices (Case Study: Alborz Province). MSc Dissertation, International Desert Research Center (IDRC), University of Tehran, 203p.

Nouri H, Anderson S, Sutton P, Beecham S, Nagler P, Jarchow CJ. 2017. NDVI, scale invariance and the modifiable areal unit problem: An assessment of vegetation in the Adelaide Parklands. Sci Total Environ 584: 11–18. https://doi.org/10.1016/j.scitotenv.2017.01.130.

Omid M, Khanali M, Zand S. 2018. Energy analysis and greenhouse gas emission in broiler farms: A case study in Alborz Province, Iran. Agric Eng Int CIGR J 19: 83–90.

Palmer WC. 1965. Meteorological drought. Research Paper No.45, U.S. Department of Commerce, Weather Bureau, Washington D.C.

Park S, Im J, Park S, Rhee J. 2017. Drought monitoring using high resolution soil moisture through multi-sensor satellite data fusion over the Korean peninsula. Agric for Meteorol 237: 257–269. https://doi.org/10.1016/j.agrformet.2017.02.022.

Pishgar-Komleh SH, Akram A, Keyhani A, VanZelm R. 2017. Life cycle energy use, costs, and greenhouse gas emission of broiler farms in different production systems in Iran-a case study of Alborz province. Environ Sci Pollut Res 24: 41–49. https://doi.org/10.1007/s11356-017-9255-3.

Rahimzadeh Bajgiran P, Darvishsefat AA, Khalili A, Makhdoum MF. 2008. Using AVHRR-based vegetation indices for drought monitoring in the Northwest of Iran. J Arid Environ 72: 1086–1096. https://doi.org/10.1016/j.jaridenv.2007.12.004.

Rhee J, Im J, Carbone GJ. 2010. Monitoring agricultural drought for arid and humid regions using multi-sensor remote sensing data. Environ Remote Sens 114: 2875-2887. https://doi.org/10.1016/j.rse.2010.07.005.

Sánchez N, González-Zamora Á, Martínez-Fernández J, Piles M, Pablos M. 2018. Integrated remote sensing approach to global agricultural drought monitoring. Agric for Meteorol 259: 141–153. https://doi.org/10.1016/j.agrformet.2018.04.022.

Sandholt I, Rasmussen K, Andersen J. 2002. A simple interpretation of the surface temperature/vegetation index space for assessment of surface moisture status. Remote Sens Environ 79: 213–224. https://doi.org/10.1016/S0034-4257(01)00274-7.

Sayago S, Ovando G, Bocco M. 2017. Landsat images and crop model for evaluating water stress of rainfed soybean. Remote Sens Environ 198: 30–39. https://doi.org/10.1016/j.rse.2017.05.008.

Shao-E Y, Bing-fang W. 2010. Calculation of monthly precipitation anomaly percentage using web-serviced remote sensing data. 2nd Int Conf Adv Computer Control 5: 621–625. https://doi.org/10.1109/ICACC.2010.5486796.

Thornthwaite CW, Mather JA, Thornthwaite W. 1955. The water balance. Publications in Climatology, Laboratory of Climatology, Vol. 8.

Tian L, Yuan S, Quiring SM. 2018. Evaluation of six indices for monitoring agricultural drought in the south-central United States. Agric for Meteorol 249: 107–119. https://doi.org/10.1016/j.agrformet.2017.11.024.

Toth C, Jóźków G. 2016. Remote sensing platforms and sensors: A survey. ISPRS J Photogramm Remote Sens 115: 22–36. https://doi.org/10.1016/j.isprsjprs.2015.10.004.

Van Loon AF, Gleeson T, Clark J, Van Dijk AIJM, Stahl K, Hannaford J. 2016. Drought in the Anthropocene. Nat Geosci 9: 89-91. https://doi.org/10.1038/ngeo2646.

Verstraeten W. 2006. Integration of remotely sensed hydrological data into an ecosystem carbon flux model. PhD Dissertation, Katholieke University Leuven, 223p.

Vicente-Serrano S, Beguería S, López-Moreno JI. 2010. A multiscalar drought index sensitive to global warming: the standardized precipitation evapotranspiration index. J Clim 23: 1696–1718. https://doi.org/10.1175/2009JCLI2909.1.

Vurukonda SSKP, Vardharajula S, Shrivastava M, Skz A. 2016. Enhancement of drought stress tolerance in crops by plant growth promoting rhizobacteria. Microbiol Res 184: 13–24. https://doi.org/10.1016/j.micres.2015.12.003.

Xu P, Zhou T, Zhao X, Luo H, Gao S, Li Z, Cao L. 2018. Diverse responses of different structured forest to drought in Southwest China through remotely sensed data. J Appl Earth Obs Geoinf Int 69: 217-225. https://doi.org/10.1016/j.jag.2018.03.009.

Xu Y, Wang L, Ross KW, Liu C, Berry K. 2018. Standardized soil moisture index for drought monitoring based on soil moisture active passive observations and 36 years of north American land data assimilation system data: A case study in the southeast United States. Remote Sens 10: 1-13. https://doi.org/10.3390/rs10020301.

Zambrano F, Lillo-Saavedra M, Verbist K, Lagos O. 2016. Sixteen years of agricultural drought assessment of the BioBío region in Chile using a 250 m resolution Vegetation Condition Index (VCI). Remote Sens 8: 1-20. https://doi.org/10.3390/rs8060530.

Zare M, Drastig K, Zude-Sasse M. 2020. Tree Water Status in Apple Orchards Measured by Means of Land Surface Temperature and Vegetation Index (LST–NDVI) Trapezoidal Space Derived from Landsat 8 Satellite Images. Sustainability 12: 1-19. https://doi.org/10.3390/su12010070.

Zargar A, Sadiq R, Naser B, Khan FI. 2011. A review of drought indices. Environ Rev 19: 333-349. https://doi.org/10.1139/a11-013.

Zhang A, Jia G. 2013. Monitoring meteorological drought in semiarid regions using multi-sensor microwave remote sensing data. Environ Remote Sens 134: 12-23. https://doi.org/10.1016/j.rse.2013.02.023.

Zhang X, Chen N, Li J, Chen Z, Niyogi D. 2017. Multi-sensor integrated framework and index for agricultural drought monitoring. Remote Sens Environ 188: 141–163. https://doi.org/10.1016/j.rse.2016.10.045.